

Short communication

## Carbon-supported Pt nanoparticles as catalysts for proton exchange membrane fuel cells

Zhaolin Liu<sup>a,\*</sup>, Leong Ming Gan<sup>a</sup>, Liang Hong<sup>a</sup>, Weixiang Chen<sup>b</sup>, Jim Yang Lee<sup>a,b</sup>

<sup>a</sup> Institute of Materials Research & Engineering, 3 Research Link, Singapore 117602, Singapore

<sup>b</sup> Department of Molecular & Chemical Engineering, National University of Singapore, 10 Kent Ridge Crescent, Singapore 119260, Singapore

Received 16 July 2004; received in revised form 19 July 2004; accepted 20 July 2004

Available online 13 September 2004

### Abstract

Pt nanoparticles supported on Vulcan XC-72 carbon and carbon nanotubes (CNTs) were prepared by a microwave-assisted polyol process. The catalysts were characterized by TEM, XRD and XPS. The Pt nanoparticles, which were uniformly dispersed on carbon, were 2–6 nm in diameter. The Pt/C catalysts prepared as such displayed the characteristic diffraction peaks of a Pt fcc structure. XPS analysis revealed that the catalysts contained mostly Pt(0), with traces of Pt(II) and Pt(IV). The electroreduction of oxygen was studied by cyclic voltammetry. It was found both Pt/C catalysts had high electrocatalytic activity in the oxygen reduction reaction. Test runs on a single stack proton exchange membrane (PEM) fuel cell showed that these electrocatalysts are very promising for fuel cell applications.

© 2004 Elsevier B.V. All rights reserved.

**Keywords:** PEM fuel cells; Catalysts; Carbon-supported Pt nanoparticles

### 1. Introduction

Pt-based electrocatalysts are usually employed in proton exchange membrane fuel cells (PEMFC) and direct methanol fuel cells (DMFC) as cathode electrocatalysts for oxygen reduction reactions in relatively low temperature. It is well known that the catalytic activity of the metal is strongly dependent on the particle shape, size and size distribution [1]. Conventional preparation techniques based on wet impregnation and chemical reduction of the metal precursors often do not provide adequate control of particle shape and size [1]. There is continuing effort to develop alternative synthesis methods based on microemulsions [2], sonochemistry [3,4], and microwave irradiation [5–8]; all of which are in principle more conducive to generating colloids and clusters on the nanoscale, and with greater uniformity.

Legratiet et al. [9] reported a significant increase in particle size when the metal content in a commercial E-TEK Pt/Vulcan catalyst is increased from 10 to 60 wt.%. The

metal particle size for a 10 wt.% Pt catalyst was 2.0 nm, but increased to 3.2 and 8.8 nm for 30 and 60 wt.% Pt catalyst, respectively. Other studies and patents [10–13] have also underlined the difficulty of using conventional methods to preparing platinum catalysts with high metal loadings (>20 wt.%) and small particle sizes (1–2 nm). In an attempt by Boennemann et al. [14], organoaluminum-stabilized bimetallic colloids with particle size smaller than 2 nm were prepared and deposited on a commercial support at room temperature. The stabilizing surfactant shell on the metal particles had to be removed before the metal particles could be used for electrocatalysis. While activated carbon is still the most common support material for electrocatalysis, new forms of carbon such as fullerenes and nanotubes, which have become more available recently, have also been investigated as catalysts support. The deposition of Pt, Ru and PtRu on carbon nanotubes (CNTs) has been reported [15–18] and the resulting supported catalysts have been superior to activated carbon-supported catalysts [19–21].

In this paper, a simple microwave-assisted polyol procedure for preparing Pt nanoparticles supported on activated carbon or CNTs is reported. The polyol process, in which

\* Corresponding author. Fax: +65 68720785.

E-mail address: [zl-liu@imre.a-star.edu.sg](mailto:zl-liu@imre.a-star.edu.sg) (Z. Liu).

an ethylene glycol solution of the metal precursor salt is slowly heated to produce colloidal metal, has recently been extended to produce metal nanoparticles supported on carbon and  $\text{Al}_2\text{O}_3$  [8,22]. In the process the polyol solution containing the metal salt is refluxed at 393–443 K to decompose ethylene glycol to yield in situ generated reducing species for the reduction of the metal ions to their elemental states. The fine metal particles produced as such may additionally be captured by a support material suspending in the solution. Conductive heating is often used but microwave dielectric loss heating may be a better synthesis option in view of its energy efficiency, speed, uniformity, and implementation simplicity [23].

## 2. Experimental

The Pt/C black (20 wt.% Pt on Cabot Vulcan XC-72) and Pt/CNT (20 wt.% Pt on carbon nanotubes synthesized by catalytic chemical vapor deposition) catalysts were prepared by microwave heating of ethylene glycol (EG) solutions of Pt salt. A typical preparation would consist of the following steps: in a 100 ml beaker, 1.0 ml of an aqueous solution of 0.05 M  $\text{H}_2\text{PtCl}_6 \cdot 6\text{H}_2\text{O}$  (Aldrich, A.C.S. Reagent) was mixed with 25 ml of ethylene glycol (Mallinckrodt, AR). 0.4 M KOH was added dropwise up to a total volume of 0.75 (or 0.25 ml). About 0.040 g of Vulcan XC-72 carbon with a specific BET surface area of  $250 \text{ m}^2 \text{ g}^{-1}$  and an average particle size of 40 nm; or CNTs prepared by chemical catalytic vapor deposition, were added to the mixture and sonicated. The beaker and its contents were heated in a household microwave oven (National NN-S327WF, 2450 MHz, 700 W) for 50 s. The resulting suspension was filtered; and the residue was washed with acetone and dried at 373 K over night in a vacuum oven.

The catalysts were examined by transmission electron microscopy (TEM) on a JEOL JEM 2010. A JEOL JSM-5600LV was used to determine the metal contents in the samples by energy dispersive X-ray analysis (EDX). For microscopic examinations the samples were first ultrasonicated in acetone for 1 h and then deposited on 3 mm Cu grids covered with a continuous carbon film. The samples were also analyzed by X-ray photoelectron spectroscopy (XPS) on a VG ESCALAB MKII spectrometer. Narrow scan photoelectron spectra were recorded for C 1s, O 1s and Pt 4f and a vendor supplied curve-fitting program (VGX900) was used for spectral deconvolution. A Philips X'Pert diffractometer using Cu  $\text{K}\alpha$  radiation and a graphite monochromator was used to obtain the powder X-ray diffraction patterns.

An EG&G Model 273 potentiostat/galvanostat, and a conventional three-electrode test cell were used for electrochemical measurements. The working electrode was a thin layer of Nafion-impregnated catalyst cast on a vitreous carbon disk held in a Teflon cylinder. The catalyst layer was obtained in the following way: (i) a slurry was first prepared by sonicating for 1 h a mixture of 0.5 ml of deionized water, 60 mg of

Pt/C catalyst, and 0.5 ml of Nafion solution (Aldrich: 5 w/o Nafion); (ii) 8  $\mu\text{l}$  of the slurry was pipetted and spread on the carbon disk; (iii) the electrode was then dried at 90 °C for 1 h and mounted on a stainless steel support. The surface area of the vitreous carbon disk was  $0.25 \text{ cm}^2$  and the catalyst loading was therefore  $1.92 \text{ mg cm}^{-2}$  based on this geometric area. Pt gauze and a saturated calomel electrode (SCE) were used as the counter and reference electrodes respectively. All potentials in this report are quoted against SCE. All electrolyte solutions were deaerated by high-purity argon for 2 h prior to any measurement. For the measurement of hydrogen electrosorption curves, the potential was cycled between +0.25 and -0.25 V at  $10 \text{ mV s}^{-1}$  to obtain the voltammograms of hydrogen adsorption in Ar-purged electrolytes. For cyclic voltammetry of methanol oxidation, the electrolyte solution was 2 M  $\text{CH}_3\text{OH}$  in 1 M  $\text{H}_2\text{SO}_4$ , which was prepared from high-purity sulfuric acid, high-purity grade methanol and distilled water.

A single stack fuel cell was assembled from a membrane/electrode assembly, two stainless steel plates with flow manifolds on the supply sides for gas and water, and two Teflon gaskets. Cell assembly is as per the description in Ref. [24]. The anode was a  $5 \text{ cm}^2$  20% Pt/C E-TEK electrode (E-TEK, Natick, MA) with a platinum loading of  $0.4 \text{ mg cm}^{-2}$ . The cathode was prepared from a suspension containing 0.0181 g (70%) of catalyst, 0.155 g (30%) of 5 w/o Nafion recast solution, and 0.5 ml of distilled  $\text{H}_2\text{O}$ , and had been ultrasonically blended for 1 h. The suspension was spread uniformly across the surface of a carbon paper substrate (Toray TGP-090). For hydrophobic treatment, the carbon paper was wetted with a 60% PTFE aqueous dispersion, followed by drying at 90 °C for 1 h and sintering at 360 °C for 30 min. For a cathode area of  $5 \text{ cm}^2$ , the amount of dried catalyst suspension (catalyst + dry Nafion) applied to the cathode was varied between 2 and  $3 \text{ mg cm}^{-2}$ . A single cell assembly was prepared by sandwiching a Nafion 117 membrane supplied by Du Pont between the anode and cathode.

## 3. Results and discussion

### 3.1. Physicochemical characterization of Pt/Vulcan carbon and Pt/CNT nanocomposites

In our approach, platinum nanoparticles are prepared and directly deposited on the carbon surface by microwave heating of ethylene glycol (EG) solutions of Pt salt. The size and composition of the alloy particles were analyzed by TEM and point resolved EDX measurements. Fig. 1a and b are typical TEM images of Vulcan carbon-supported and CNT-supported catalysts, showing a remarkably uniform and high dispersion of metal particles on the carbon surface. The particle size distributions of the metal in the supported catalysts were obtained by directly measuring the size of 150 randomly chosen particles in the magnified TEM images (e.g. Fig. 1c for the Pt-Vulcan carbon sample). The average

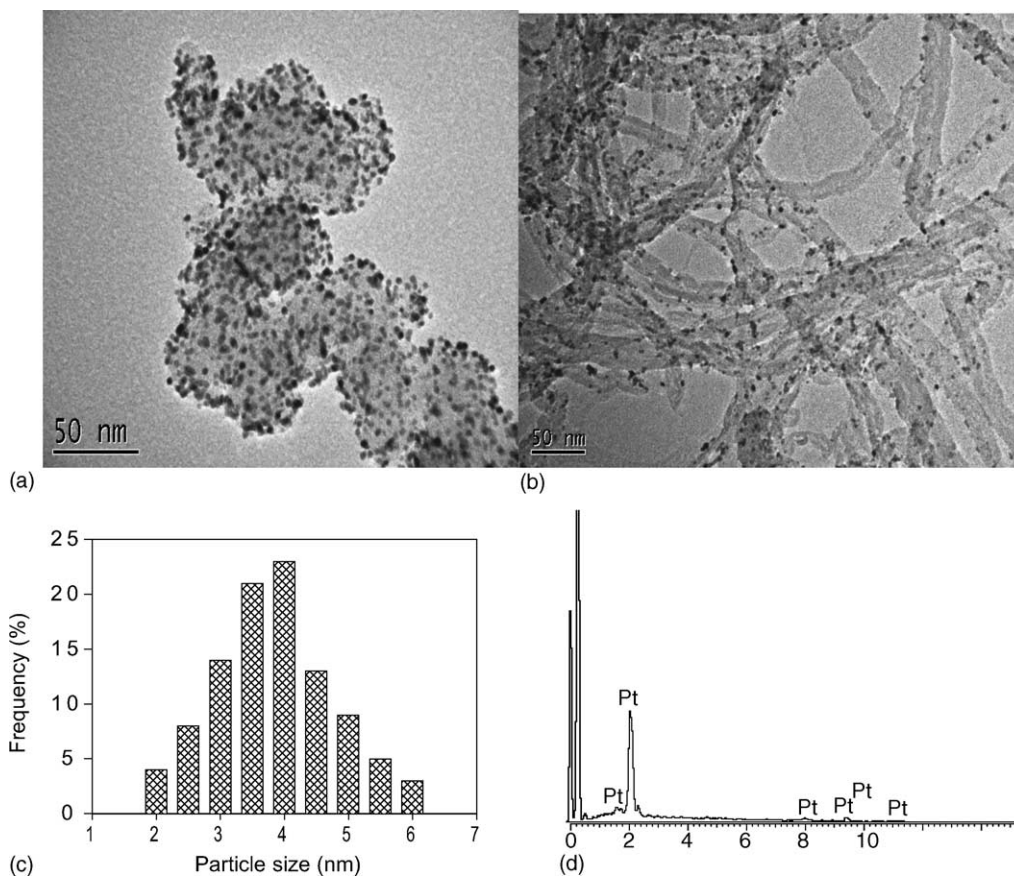


Fig. 1. TEM images of microwave-synthesized Pt nanoparticles supported on different carbon: (a) Vulcan XC-72 carbon; (b) carbon nanotubes (nominal Pt loading 20 wt.%); (c) particle size distribution for the Pt/Vulcan carbon; (d) EDX spectra of Vulcan carbon-supported Pt nanoparticles.

diameters of  $3.8 \pm 0.3$  nm for Pt/Vulcan carbon and  $3.6 \pm 0.3$  nm for Pt/CNT were accompanied by relatively narrow particle size distributions (2–6 nm). The microwave-assisted heating of  $\text{H}_2\text{PtCl}_6/\text{KOH}/\text{H}_2\text{O}$  in ethylene glycol had evidently facilitated the formation of smaller and more uniform Pt particles and their dispersion on either the Vulcan carbon or CNT support. It is generally agreed that the size of metal nanoparticles is determined by the rate of reduction of the metal precursor. The dielectric constant (41.4 at 298 K) and the dielectric loss of ethylene glycol are high, and hence rapid heating occurs easily under microwave irradiation. In ethylene glycol mediated reactions (the ‘polyol’ process), ethylene glycol also acts as a reducing agent to reduce the metal ion to metal powders. The fast heating by microwave accelerates the reduction of the metal precursor and the nucleation of the metal clusters. The easing of the nucleation-limited process greatly assists in small particle formation. Additionally the homogeneous microwave heating of liquid samples reduces the temperature and concentration gradients in the reaction medium, thus providing a more uniform environment for the nucleation and growth of metal particles. The carbon surface may contain sites suitable for heterogeneous nucleation and the presence of a carbon surface interrupts particle growth. The smaller and nearly single dispersed Pt nanoparticles on carbon XC-72 prepared by microwave irradiation

can be rationalized in terms of these general principles. EDX measurements (Fig. 1d) showed Pt contents of 18.9 wt.% for Pt/Vulcan carbon and 19.4 wt.% for Pt/CNT.

The powder XRD patterns for Pt/Vulcan carbon and Pt/CNT are shown in Fig. 2 alongside the diffraction patterns of a Vulcan carbon-supported Pt catalyst used as comparison.

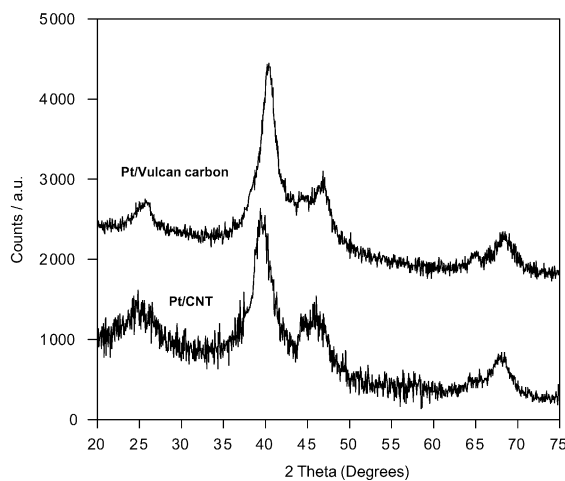


Fig. 2. XRD patterns of microwave-synthesized Pt/Vulcan carbon and Pt/CNT catalysts.

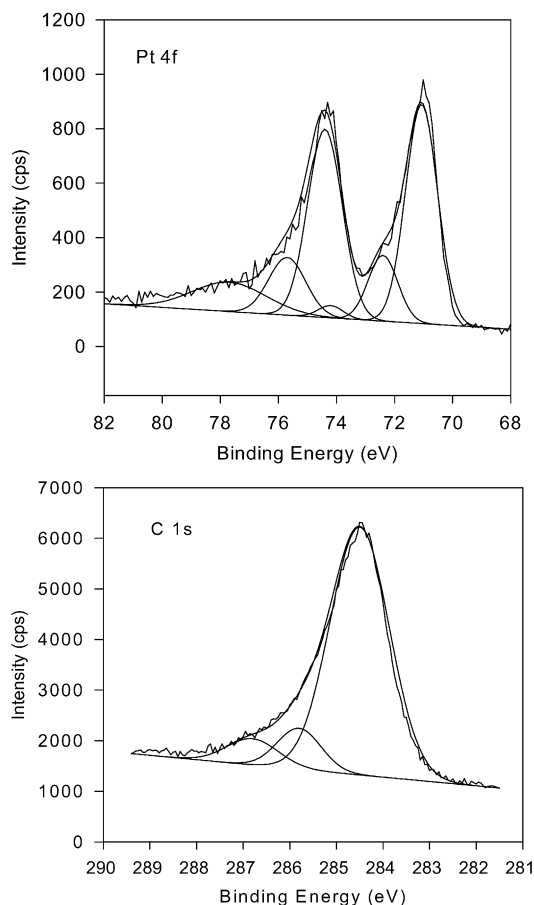


Fig. 3. The Pt 4f and C 1s regions of the XPS spectrum of the Pt/Vulcan carbon catalyst.

Both Pt/Vulcan carbon and Pt/CNT electrocatalysts displayed the characteristic patterns of Pt fcc diffraction. The  $2\theta$  values of the (1 1 1) peak for Pt/Vulcan carbon and Pt/CNT were  $39.85^\circ$  and  $39.95^\circ$ , respectively. The Pt(2 2 0) diffraction was  $67.60^\circ$  for Pt/Vulcan carbon,  $67.65^\circ$  for Pt/CNT. The broader diffraction peaks for the two catalysts also led to smaller average alloy particle size as calculated by the Scherrer equation [25]:

$$L = \frac{0.9\lambda_{K\alpha_1}}{(B_{2\theta} \cos \theta_B)}$$

where  $L$  is the average particle size,  $\lambda_{K\alpha_1}$  the X-ray wavelength ( $1.54056 \text{ \AA}$  for Cu  $K\alpha_1$  radiation),  $B_{2\theta}$  the peak broadening and  $\theta_B$  the angle corresponding to the peak maximum. The calculation results, which estimated the average size of  $3.9 \pm 0.3 \text{ nm}$  for Pt/Vulcan carbon and  $3.7 \pm 0.3 \text{ nm}$  for Pt/CNT, are in good agreement with the TEM measurements. Besides a small shift to a slightly higher value, X-ray scattering from the CNT support was similar to Vulcan carbon and was detectable around  $2\theta = 24\text{--}26^\circ$ .

XPS was used to determine the surface oxidation states of the metals. As most of the atoms in small particle clusters are surface atoms, the oxidation state measured as such would also reflect well the bulk oxidation state. Fig. 3 shows the Pt 4f

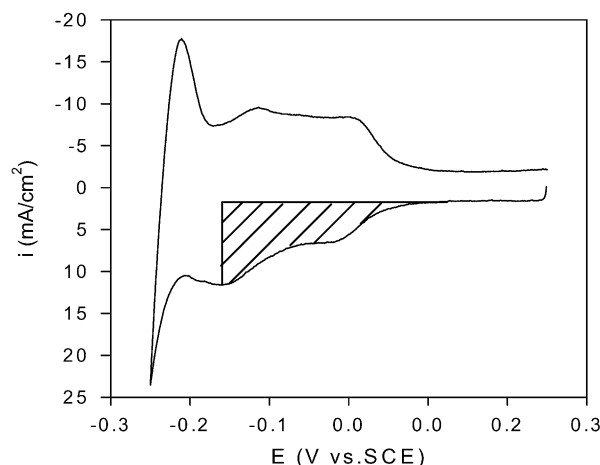


Fig. 4. Hydrogen electroadsorption voltammetric profiles for the microwave-synthesized Pt/CNT catalysts in 1 M  $\text{H}_2\text{SO}_4$  with a scan rate of  $50 \text{ mV s}^{-1}$  at room temperature. The hatched area represents the amount of charge of the electroadsorption of hydrogen on Pt.

and C 1s regions of the XPS spectrum of the Pt/Vulcan carbon catalyst. The Pt 4f signal consisted of three pairs of doublets. The most intense doublet ( $71.07$  and  $74.4 \text{ eV}$ ) was due to metallic Pt. The second set of doublets ( $72.4$  and  $75.7 \text{ eV}$ ), which was observed at BE  $1.4 \text{ eV}$  higher than Pt(0), could be assigned to the Pt(II) chemical state as in PtO and Pt(OH)<sub>2</sub> [26]. The third doublet of Pt was the weakest in intensity, and occurred at even higher BEs ( $74.2$  and  $77.7 \text{ eV}$ ). These are the indications that they were most likely caused by a small amount of Pt(IV) species on the surface. The slight shift in the Pt(0) peak to higher binding energies is a known effect for small particles, as has been reported by Roth et al. [27]. The C 1s spectrum appears to be composed of graphitic carbon ( $284.6 \text{ eV}$ ) and  $\text{--C=O}$  like species ( $285.83 \text{ eV}$ ) [26]. A small amount of surface functional groups with high oxygen contents was also noted in the spectrum ( $286.8 \text{ eV}$ ).

### 3.2. Electrochemical performances

The real surface area of platinum for the Pt/Vulcan carbon and Pt/CNT catalysts could be estimated from the integrated charge in the hydrogen absorption region of the cyclic voltammogram (hatched area in Fig. 4). The areas in  $\text{m}^2 \text{ g}^{-1}$  were calculated from the following formula assuming a correspondence value of  $0.21 \text{ mC cm}^{-2}$  (calculated from the surface density of  $1.3 \times 10^{15} \text{ atom cm}^{-2}$ , a value generally admitted for polycrystalline Pt electrodes [28]) and the Pt loading.

$$A_{\text{EL}}(\text{m}^2 \text{ g}_{\text{cat}}^{-1}) = Q_{\text{H}} / (0.21 \times 10^{-3} \text{ C g}_{\text{cat}}^{-1})$$

The calculation results were shown in Table 1. All measurements are made with the near same catalyst loading at  $0.25 \text{ cm}^2$  disk electrode. The use of Vulcan carbon or CNT did not result in significant differences in the Pt surface area. This is not surprising in view of the similarly small metal particle size in these supported metallic systems.



Table 1

The real (active) surface areas of Pt/Vulcan carbon and Pt/CNT catalysts as determined by hydrogen electroadsorption

Origin of Pt/C catalyst	$Q_H^a$ (mC)	$S_{EL}^b$ (cm <sup>2</sup> )	Catalyst loading (mg/0.25 cm <sup>2</sup> )	$A_{EL}^c$ (m <sup>2</sup> g <sub>cat</sub> <sup>-1</sup> )
Pt/Vulcan carbon	10.8	51.4	0.42	12.2
Pt/CNT	10.4	49.5	0.43	11.5

<sup>a</sup>  $Q_H$ : charges exchanged during the electroadsorption of hydrogen on Pt.<sup>b</sup>  $S_{EL}$ : real surface area obtained electrochemically.<sup>c</sup>  $A_{EL}$ : real surface area obtained electrochemically per gram of catalyst.

The Pt/Vulcan carbon and Pt/CNT catalysts were tested for their electrocatalytic activity in oxygen reduction reaction, which is important in fuel cell applications [29,30]. Background cyclic voltammograms were collected in 0.5 M H<sub>2</sub>SO<sub>4</sub>, for a glassy carbon (GC) electrode and a CNT pasted electrode of the same geometric area (Fig. 5a). From the increase in the capacitive current it is obvious that the CNT electrode had a higher active surface area than a typical GC electrode [30–32] in the potential range investigated. In the absence of the Pt nanoparticles, no O<sub>2</sub> reduction was observed in this potential window. Fig. 5b compares the O<sub>2</sub> reduction currents of Pt/Vulcan carbon and Pt/CNT catalysts in a 0.5 M H<sub>2</sub>SO<sub>4</sub> electrolyte saturated with oxygen. For the Pt/Vulcan carbon and Pt/CNT catalysts, a very large O<sub>2</sub> reduction wave

was detected between 0.1 and 0.5 V, characteristic of Pt-based electrocatalysis in this solution. The large cathodic current indicates high electrocatalytic activity of the Pt/Vulcan carbon and Pt/CNT electrode in the oxygen reduction reaction.

The performances of the electrocatalysts in a real fuel cell are shown in Fig. 6. The polarization curves were obtained from a single stack PEM fuel cell using the same type of anode. The activities of oxygen reduction for Pt/Vulcan carbon and Pt/CNT electrodes seem quite similar.

In the low current density region, the voltage drop in the potential–current curve, generally known as activation polarization, reflects the sluggish kinetics intrinsic to the oxygen reduction reaction at the cathode surface. The linear decrease in voltage in the mid-to-high current density range, or ohmic polarization, arises from limitations in proton transport through the electrolyte membrane from anode to cathode, and/or limitations in electron-flow in the electrode materials.

The experimental polarization data may be analyzed using the semi-empirical equation proposed of Srinivasan and co-workers [33]:

$$E = E^\circ - b \log i - Ri \quad (1)$$

where

$$E^\circ = E_r + b \log i^\circ \quad (2)$$

$E$  and  $i$  are experimentally measured cell voltage and current,  $E_r$  the reversible cell voltage,  $i^\circ$  and  $b$  are the exchange current and the Tafel slope for oxygen reduction, respectively.  $R$  represents the total dc resistance; a summation of resistances

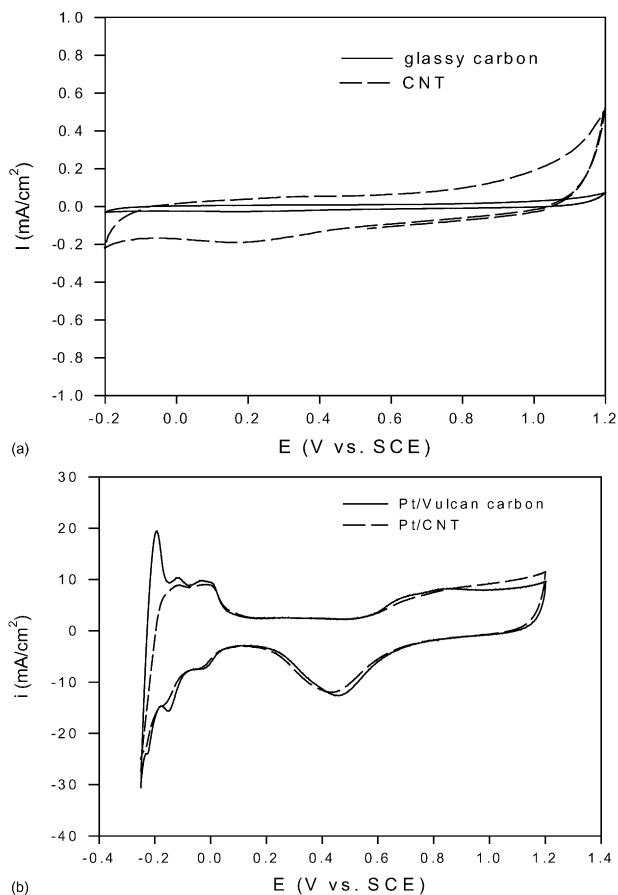


Fig. 5. Voltammograms of (a) glass carbon and pasted CNT electrodes and (b) pasted electrodes of Pt/Vulcan carbon and Pt/CNT in 1 M H<sub>2</sub>SO<sub>4</sub> with a scan rate of 50 mV s<sup>-1</sup> at room temperature.

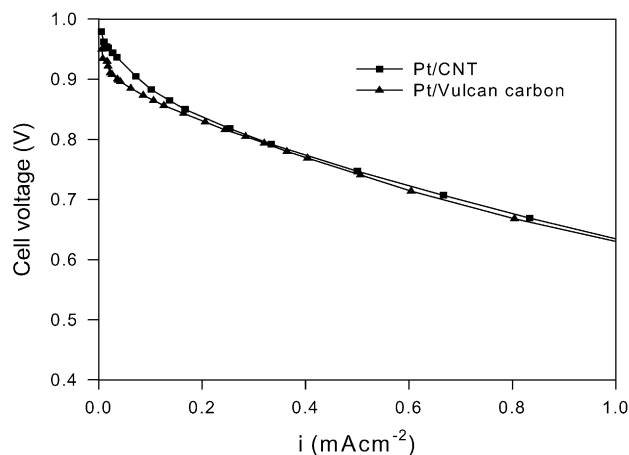


Fig. 6. Polarization curves of Pt/CNT and Pt/Vulcan carbon electrocatalysts from a PEM test cell. O<sub>2</sub>: 1 bar, H<sub>2</sub>: 1 bar, 50 °C.

Table 2  
Kinetic parameters from regression analysis of polarization

Catalysts	$E^{\circ}$ (V)	$b$ (V dec <sup>-1</sup> )	$R$ ( $\Omega$ cm <sup>2</sup> )	$E_r$ (V)	$i^{\circ}$ (mA cm <sup>-2</sup> )
Pt/CNT	0.836	0.067	0.208	1.081	$2.19 \times 10^{-4}$
Pt/Vulcan carbon	0.836	0.051	0.212	1.035	$1.25 \times 10^{-4}$

in the polymer membrane and other electrode components accountable for the linear variation of potential with current. The electrochemical process according to Eq. (1) is therefore only rate-limited by activation and ohmic polarizations.

The experimental data were fitted to the above equations by a nonlinear least squares method. The fit was good as is shown by the solid regression lines in Fig. 6. The kinetic parameters of the two electrocatalysts from regression analysis are summarized in Table 2. The two electrocatalysts have shown similar  $b$  values of ca. 0.06 V which is common to most supported and unsupported Pt electrodes [34]. Since no deviation from linearity was noticed even at the high current density end of the polarization curves, there was no intrusion of mass transfer effects. The two electrocatalysts have also shown similar exchange current density per unit geometric area ( $i^{\circ}$ ).

#### 4. Conclusions

A microwave-assisted rapid heating method was used to prepare carbon-supported Pt nanoparticles as cathode electrocatalysts for oxygen reduction reactions in PEM fuel cell. The preparation method is simple, fast and energy-efficient, and can be used as a general method of preparation for other supported metal system where the metal precursors are susceptible to the polyol process. The Pt nanoparticles, which were uniformly dispersed on carbon, were 2–6 nm in diameters. Both Pt/C catalysts prepared as such displayed the diffraction patterns of the Pt fcc structure. XPS analysis revealed that the catalysts contained mostly Pt(0), with traces of Pt(II) and Pt(IV). The microwave-prepared catalysts showed high electrocatalytic activity for oxygen reduction as tested by a single stack PEM fuel cell.

#### References

- [1] I.S. Armadi, Z.L. Wang, T.C. Green, A. Henglein, M.A. El-Sayed, *Science* 272 (1924) 1996.
- [2] Z.L. Liu, J.Y. Lee, M. Han, W.X. Chen, L.M. Gan, *J. Mater. Chem.* 12 (2002) 2453.
- [3] K. Okitsu, A. Yue, S. Tanabe, H. Matsumoto, *Chem. Mater.* 12 (2000) 3006.
- [4] T. Fujimoto, S. Teraushi, H. Umehara, I. Kojima, W. Henderson, *Chem. Mater.* 13 (2001) 1057.
- [5] W.Y. Yu, W.X. Tu, H.F. Liu, *Langmuir* 15 (1999) 6.
- [6] W.X. Yu, H.Y. Liu, *Chem. Mater.* 12 (2000) 564.
- [7] S. Komarneni, D.S. Li, B. Newalkar, H. Katsuki, A.S. Bhalla, *Langmuir* 18 (2002) 5959.
- [8] W.X. Chen, J.Y. Lee, Z.L. Liu, *Chem. Commun.* (2002) 2588.
- [9] B. Legratiet, H. Remita, G. Picq, M.O. Delcourt, *J. Catal.* 164 (1996) 36.
- [10] A. Gamez, D. Richard, P. Gallezot, F. Gloaguen, R. Faure, R. Durand, *Electrochim. Acta* 41 (1996) 307.
- [11] M. Watanabe, K. Sakairi, US Patent 5,728,485 (1998).
- [12] K. Tsurumi, P. Stonehart, US Patent 5,480,851 (1995).
- [13] P. Stonehart, US Patent 5,593,934 (1997).
- [14] H. Boennemann, R. Binkmann, P. Britz, U. Endruschat, R. Moertel, U.A. Paulus, G.J. Feldmeyer, T.J. Schmidt, H.A. Gasteiger, R.J. Behm, *J. New Mater. Electrochem. Syst.* 3 (2000) 199.
- [15] B. Xue, P. Chen, Q. Hong, J.Y. Lin, K.L. Tan, *J. Mater. Chem.* 11 (2001) 2387.
- [16] R.Q. Yu, L.W. Chen, Q.P. Liu, J.Y. Lin, K.L. Tan, S.C. Ng, H.S.O. Chan, G.Q. Xu, T.S.A. Hor, *Chem. Mater.* 10 (1998) 718.
- [17] B. Rajesh, K.R. Thampi, J.M. Bonard, B. Viswanathan, *J. Mater. Chem.* 10 (2000) 1575.
- [18] V. Lordi, N. Yao, J. Wei, *Chem. Mater.* 13 (2001) 733.
- [19] J.M. Planeiz, N. Coustel, B. Coq, V. Brotons, P.S. Kumbhar, R. Dutartre, P. Geneste, P. Bernier, P.M. Ajayan, *J. Am. Chem. Soc.* 116 (1994) 7395.
- [20] Z.L. Liu, X. Lin, J.Y. Lee, W. Zhang, M. Hang, L.M. Gan, *Langmuir* 18 (2002) 4054.
- [21] W.Z. Li, C.H. Liang, J.S. Qiu, W.J. Zhou, H.M. Han, Z.B. Wei, G.Q. Sun, Q. Xin, *Carbon* 40 (2002) 791.
- [22] A. Miyazaki, I. Balint, K.I. Aika, Y. Nakano, *J. Catal.* 203 (2001) 364.
- [23] S.A. Galema, *Chem. Soc. Rev.* 26 (1997) 233.
- [24] Z. Shao, B. Yi, M. Han, *J. Power Sources* 79 (1999) 82.
- [25] B.E. Warren, *X-ray Diffraction*, Addison-Wesley, Reading, MA, 1996.
- [26] A.K. Shukla, M.K. Ravikumar, A. Roy, S.R. Barman, D.D. Sarma, A.S. Aricò, V. Antonucci, I. Pino, N. Giordano, *J. Electrochem. Soc.* 141 (1994) 1517.
- [27] C. Roth, M. Goetz, H. Fuess, *J. Appl. Electrochem.* 31 (2001) 793.
- [28] R. Woods, *J. Electroanal. Chem.* 9 (1976) 1.
- [29] J.O'M. Bockris, S. Srinivasan, *Fuel Cell, Their Electrochemistry*, McGraw-Hill, New York, 1969.
- [30] K. Kinoshita, *Carbon, Electrochemical and Physico Chemical Properties*, Wiley, New York, 1988.
- [31] A. Tomita, Y. Tamai, *J. Phys. Chem.* 75 (1971) 649.
- [32] F. Gloaguen, J.M. Leger, C. Lamy, *J. Appl. Electrochem.* 9 (1997) 1052.
- [33] E.A. Ticianelli, C.R. Derouin, A. Redondo, S. Srinivasan, *J. Electrochem. Soc.* 135 (1988) 2209.
- [34] A. Parthasarathy, S. Srinivasan, A.J. Appleby, C.R. Martin, *J. Electroanal. Chem.* 339 (1992) 101.